Evidence for reduced collectivity around the neutron mid-shell in the stable even-mass Sn isotopes from new lifetime measurements

A. Jungclaus [a,*], J. Walker [a,b], J. Leske [c], K.-H. Speidel [d], A.E. Stuchbery [e], M. East [e], P. Boutachkov [f],
J. Cederkäll [g], P. Doornenbal [h], J.L. Egido [b], A. Ekström [g], J. Gerl [f], R. Gernhäuser [i], N. Goel [f], M. Górska [f],
I. Kojouharov [f], P. Maier-Komor [i], V. Modamio [a,b], F. Naqvi [j,f], N. Pietralla [c], S. Pietri [k,f], W. Prokopowicz [f],
H. Schaffner [f], R. Schwengner [l], H.-J. Wollersheim [f]

[a] Instituto de Estructura de la Materia, CSIC, E-28006 Madrid, Spain
[b] Departamento de Física Teórica, Universidad Autónoma de Madrid, E-28049 Madrid, Spain
[c] Institut für Kernphysik, Technische Universität Darmstadt, D-64289 Darmstadt, Germany
[d] Helmholtz-Institut für Strahlen- und Kernphysik, Universität Bonn, D-53115 Bonn, Germany
[e] Department of Nuclear Physics, Australian National University, Canberra ACT 0200, Australia
[f] Gesellschaft für Schwerionenforschung (GSI), D-64291 Darmstadt, Germany
[g] Department of Physics, Lund University, S-22100 Lund, Sweden
[h] RIKEN Nishina Center, Wako, Saitama 351-0198, Japan
[i] Physik Department E12, Technische Universität München, D-85748 Garching, Germany
[j] Institut für Kernphysik, Universität zu Köln, D-50937 Köln, Germany
[k] Department of Physics, University of Surrey, Guildford, GU2 7XH, United Kingdom
[l] Institut für Strahlenphysik, FZ Dresden-Rossendorf, D-01314 Dresden, Germany

ARTICLE INFO

ABSTRACT

Precise measurements of the lifetimes of the first excited 2^+ states in the stable even-A Sn isotopes $^{112-124}$Sn have been performed using the Doppler shift attenuation technique. For the isotopes ^{112}Sn, ^{114}Sn and ^{116}Sn the $E2$ transition strengths deduced from the measured lifetimes are in disagreement with the previously reported values and indicate a shallow minimum at $N = 66$. The observed deviation from a maximum at mid-shell is attributed to the obstructive effect of the $s_{1/2}$ neutron orbital in generating collectivity when near the Fermi level.

The chain of semi-magic tin isotopes occupies an exceptional position in nuclear structure research. With the 33 experimentally accessible isotopes between the two double-magic cornerstones ^{100}Sn and ^{132}Sn, it allows for systematic and stringent tests of the validity of nuclear structure models across an entire span of a large major neutron shell, from the proton dripline with $N = Z$ to the isotope which has eight neutrons more than the most neutron-rich stable tin isotope. While the regions around the double-magic isotopes are of fundamental importance for the understanding of the nuclear structure far away from the valley of stability [1–3] the possibility to follow quantities such as excitation energies and transition strengths over a large range of neutron to proton ratios,

namely $N/Z = 1.0$–1.64, enables the scrutiny of basic concepts in nuclear structure physics.

There is a general understanding that the collectivity in atomic nuclei is highest when the number of nucleons outside closed shells is largest, i.e. around mid-shell. A formal rationale for this general rule is provided by the seniority scheme, which supplies an exact solution to the simple pairing Hamiltonian for one single j-shell. It predicts a constant excitation energy for the first excited 2^+ state and a parabolic behavior with the maximum value at mid-shell of the transition probabilities to these first-excited 2^+ states, $B(E2; 0^+_{g.s.} \rightarrow 2^+_1)$ (in the following abbreviated as $B(E2)$), as a function of the number of particles in this j-shell [4]. Some features of this simple seniority model remain effective even when it is generalized by considering several j orbitals and more realistic interactions [4]. Because of the strong pairing correlations along the tin isotopic chain, it has long been considered as a good

example for the approximate validity of the generalized seniority scheme. Indeed, the energy of the first excited 2^+ state is near constant across the entire major $N = 50$–82 neutron shell and at least in its upper half the $B(E2)$ values decrease with increasing neutron number from the mid-shell nucleus ^{116}Sn toward the $N = 82$ shell closure following a smooth parabolic behavior as described also by seniority truncated large scale shell model calculations [5–7].

In recent years, however, a series of experiments have examined the $E2$ strength in the Sn isotopes with $A = 106$–114, in the lower half of the major neutron shell [7–13]. In these studies on stable and neutron-deficient isotopes, an increase in $E2$ strengths has been observed between the mid-shell isotope ^{116}Sn and its neighbor ^{114}Sn, with the values then staying nearly constant within the experimental uncertainties down to ^{106}Sn. This behavior contrasts with predictions from modern large-scale shell model calculations [7].

The measured $E2$ transition strengths in the stable even-A Sn isotopes are mainly based on Coulomb excitation experiments while information from direct lifetime measurements is scarce. We have measured the 2^+_1 state lifetimes in all of the stable even-A Sn isotopes using the Doppler-shift attenuation (DSA) method in order to provide an independent evaluation of the observed discontinuity in the $B(E2)$ systematics between ^{114}Sn and ^{116}Sn.

Two new experiments, with virtually identical experimental setups, were performed at the UNILAC accelerator of the Gesellschaft für Schwerionenforschung (GSI). In addition, we have analyzed data obtained in a recent magnetic moment measurement [14] at the Australian National University (ANU). At GSI 4.0 MeV/u beams of ^{112,114,116}Sn were used in the first run and a 3.8 MeV/u ^{122}Sn beam was used in the second. Besides the lifetime measurement we were aiming to determine the magnetic moments of the 2^+_1 states using the transient field technique (the magnetic moment results will be presented elsewhere [15]); the beam particles therefore impinged on multilayer targets consisting of 0.67 mg/cm^2 (0.66 mg/cm^2 in the ^{122}Sn run) natural C, 10.8 (10.9) mg/cm^2 natural Gd, 1.0 (1.0) mg/cm^2 Ta and finally a 4.86 (5.23) mg/cm^2 Cu layer. A thick Ta foil was mounted behind the target to stop the beam. Four Si diodes (1 cm × 1 cm each) were placed 30 mm (27 mm) downstream above and below the beam axis to detect the forward scattered C target ions in the vertical angular ranges of 2°–20° and 23°–38°. The γ rays emitted from the excited states populated in the Coulomb excitation of the Sn projectiles on the C target layer were detected in coincidence with the C ions in four EUROBALL cluster detectors positioned in a horizontal plane at angles of ±65° and ±115° with respect to the beam axis at a distance of 24 cm (22 cm) from the target. Each of the cluster detectors consists of seven individual Ge crystals, which for the lineshape analysis have been combined into groups according to their average polar angle with respect to the beam. For the lifetime determination the spectra obtained with the detectors positioned at 53°, 65°, 115° and 127° to the beam axis have been analyzed because at these angles the lineshapes are most sensitive to the lifetime value.

To analyze the observed Doppler-broadened lineshapes and extract the lifetime information we modified the LINESHAPE program package [16] in order to (i) evaluate the kinematics of the Coulomb excitation reaction, taking into account the non-cylindrical geometry of the particle detectors, (ii) take into account the structure of the multilayer targets, and (iii) include angular correlation effects. For the description of the slowing-down process the stopping powers of Ziegler et al. [17] were used. Since the experiments at GSI were performed at relatively high beam energies, additional excited states above the first 2^+ states of interest were populated. Thus feeding into the 2^+_1 state from the higher states, mainly from
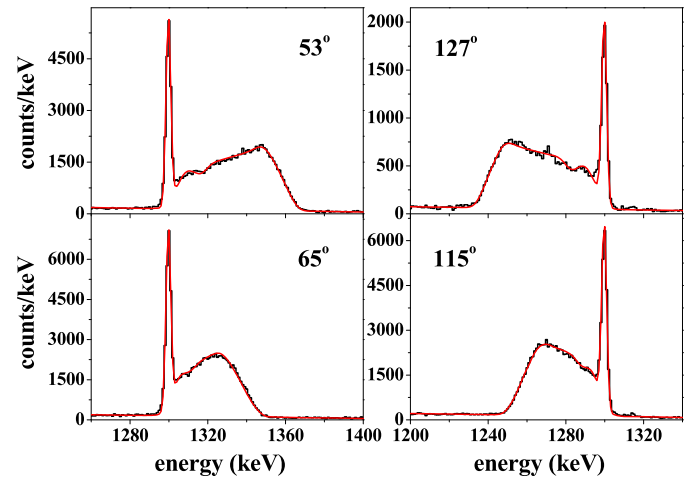

Fig. 1. Lineshape fits for the $2^+_1 \to 0^+$ transition in ^{114}Sn observed in the Ge crystals at the designated polar angles with respect to the beam axis, in coincidence with C ions.

the 4^+_1 and 3^-_1 levels, has to be taken into account in the analysis of the lineshapes. For each isotope under study the feeding intensities were determined from the γ ray spectra taking into account angular correlation effects. This observed feeding, which amounts to 5–15% from the 4^+_1 and 15–30 % from the 3^-_1 levels, respectively, has been included in the fits to the lineshapes of the $2^+_1 \to 0^+$ transitions. While the 4^+_1 states are too long lived to show a significant Doppler shifted fraction, the 3^-_1 states are shorter-lived and their lifetimes have been determined from the lineshapes of the $3^-_1 \to 2^+_1$ transitions.

For each transition of interest eight different experimental lineshapes corresponding to the combinations of the four γ-ray detection angles with the two pairs of Si detectors covering different angular ranges have been analyzed. As an example of the lineshape analysis, Fig. 1 shows the fits obtained for the $2^+_1 \to 0^+$ ground state transition in ^{114}Sn in the spectra taken at 53°, 65°, 115° and 127° to the beam axis in coincidence with C ions detected in the inner pair of Si detectors. Note that the lineshapes obtained at symmetric angles in forward and backward direction, 65°/115° and 53°/127°, are not perfectly symmetric due to the initial recoil velocity being more than 7% of the velocity of light; relativistic effects must be included in the fitting procedure.

To consider the uncertainties introduced by the feeding contributions for the 2^+_1 state, the intensities of both the $4^+_1 \to 2^+_1$ as well as $3^-_1 \to 2^+_1$ feeding transitions were varied independently by ±20% and the resulting variation of the deduced 2^+_1 lifetime was added to the statistical error. Final lifetime values were obtained as weighted means of the eight individual fit results. Uncertainties in the stopping power description of about 5% have been considered in the determination of the quoted error. The results obtained for both $\tau(3^-_1)$ and $\tau(2^+_1)$ in ^{112,114,116,122}Sn from the two GSI experiments are summarized in Table 1. It is noteworthy that the lifetimes of the 3^-_1 states in ^{116}Sn and ^{122}Sn determined in the present work are in good agreement with the literature values [18,19].

To test the robustness of the lifetime results we performed a number of checks using ^{114}Sn as an example. To test the importance of an exact knowledge of the thicknesses of the various target layers, the thickness of the Gd and Ta layers were varied independently by ±0.5 mg/cm^2. The obtained lifetime values were all within 0.01 ps with the best fits obtained for the nominal thicknesses. This observed independence of the fitted lifetime on the Gd and Ta thicknesses is expected since the decay of the 2^+_1 state

Table 1

Lifetimes of the 2^+_1 and 3^-_1 states and the $B(E2; 0^+_{g.s.} \to 2^+_1)$ transition probabilities in $^{112-124}$Sn determined in the present work compared to the adopted literature values [5].

Nucleus	$E(2^+_1)$ (keV)	$\tau(3^-_1)$ (ps)		$\tau(2^+_1)$ (ps)			$B(E2; 0^+_{g.s.} \to 2^+_1)$ (e^2b^2)			
		GSI	Previous	GSI	ANU	Previous	GSI	ANU	Previous	Renorm.[1]
^{112}Sn	1257	0.31(2)	–	0.65(4)	–	0.537(18)[2]	0.200(12)	–	0.242(8)[2]	0.195(8)
^{114}Sn	1300	0.52(3)	–	0.60(4)	–	0.474(16)[3]	0.183(12)	–	0.232(8)[3]	0.186(8)
^{116}Sn	1294	0.48(3)	0.49(6)[4]	0.66(4)	0.68(4)	0.539(15)	0.170(10)	0.165(10)	0.209(6)	
^{118}Sn	1230	–	–	–	0.79(4)	0.695(27)	–	0.183(9)	0.209(8)	
^{120}Sn	1171	–	–	–	0.97(5)	0.916(19)	–	0.191(10)	0.202(4)	
^{122}Sn	1141	0.13(2)	0.114$\left(^{+7}_{-4}\right)$[4]	1.29(8)	–	1.101(23)	0.164(10)	–	0.192(4)	
^{124}Sn	1132	–	–	–	1.48(15)	1.324(32)	–	0.148(15)	0.166(4)	

[1] Previous values from [12,13] renormalized to the new GSI results.

[2] The more precise values from [13] are quoted here instead of $B(E2; 0^+ \to 2^+_1) = 0.240(14)$ e^2b^2 and $\tau = 0.544(32)$ ps [5].

[3] The more precise values from [12] are quoted here instead of $B(E2; 0^+ \to 2^+_1) = 0.24(5)$ e^2b^2 and $\tau = 0.48(10)$ ps [5].

[4] From Refs. [18] and [19].

in most cases takes place well before the recoiling Sn ion reaches the Gd–Ta interface. And whenever the 2^+_1 state had been populated from the long-lived 4^+_1 state it decays after the ion has been completely stopped in the Cu layer. This means that possible variations of the layer thicknesses have no influence on the obtained lifetimes. In a second step we varied the region of the lineshape considered in the fit. Choosing only the region of largest Doppler shifts corresponds to selecting the highest recoil velocities and the first layer of the backing. However, no changes in the resulting lifetime values were found (variations within 0.01 ps) for many different widths and positions of the fit region. Finally, to check the influence of the choice of the stopping power used in the lineshape analysis on the resulting lifetime values the analysis was repeated by replacing the Ziegler stopping powers with those of Northcliffe–Schilling (NS) [20]. The resulting lifetimes were again within 0.01 ps which indicates that for Gd as stopping material and the large recoil velocities relevant in this analysis both parametrizations are very similar. For a more detailed discussion of the full analysis procedure we refer the reader to a forthcoming publication [21].

The ANU measurement used a 190-MeV ^{58}Ni beam provided by the ANU 14UD Pelletron accelerator and Coulomb excited the natural Sn layer of a multilayer target (0.06 mg/cm^2 natural Pd, 0.73 mg/cm^2 natural Sn, 4.7 mg/cm^2 Fe, 2.07 mg/cm^2 In and 12.5 µm Cu). The γ rays deexciting the first-excited 2^+ states in the even $^{116-124}$Sn isotopes were observed by four Ge detectors placed at $\pm 65°$ and $\pm 115°$ with respect to the beam axis in coincidence with backscattered ^{58}Ni ions. For further details concerning the experiment see Ref. [14]. The lineshapes of the $2^+_1 \to 0^+$ transitions were analyzed using the same approach as described above for the GSI data with the only difference that it is now the target ion which is Coulomb excited and not the projectile. Since only the first 2^+ states were excited in this experiment, and therefore no feeding corrections need be applied in the lineshape analysis, the determination of $\tau(2^+_1)$ in ^{116}Sn from the ANU data provides an independent check of the procedure used in the analysis of the GSI data, in particular of the sidefeeding corrections. Fig. 2 shows the relevant part of the γ ray spectrum observed in the detectors positioned at $\pm 65°$. For the overlapping lines corresponding to the $2^+_1 \to 0^+$ transitions in ^{122}Sn and ^{124}Sn we assumed a value of $\tau = 1.29(8)$ ps for the 2^+_1 state in ^{122}Sn, as obtained from the GSI data (see Table 1), and then determined the 2^+_1 lifetime in ^{124}Sn to be $\tau = 1.48(15)$ ps. Note that in the case of the ANU data, the use of Northcliffe–Schilling instead of Ziegler's stopping powers leads to slightly worse descriptions of the lineshapes and a decrease of about 0.03–0.04 ps in the resulting lifetimes.

With the results summarized in Table 1, directly measured lifetime values for the 2^+_1 states are now available for all stable even-A Sn isotopes. Comparing the $B(E2)$ values derived from
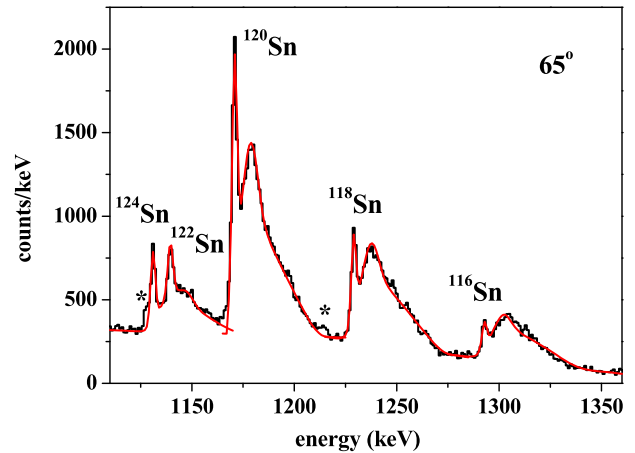

Fig. 2. Lineshape fits of the $2^+_1 \to 0^+$ transitions in ^{116,118,120,124}Sn in the spectrum observed in the Ge detectors positioned at $\pm 65°$ from the experiment performed at the Australian National University [14]. Stars label two contaminating transitions in ^{106}Pd and ^{110}Pd.

these lifetimes to the literature values [5,12,13] systematically lower values were found in all cases with the discrepancy being largest for ^{112}Sn, ^{114}Sn and ^{116}Sn. We emphasize here the robustness of the new data, particularly for revealing systematic trends, and also the absolute values. In ^{116}Sn, our present value of $B(E2) = 0.168(7)$ e^2b^2, which is based on the two independent lifetime values obtained from the GSI and ANU data, is about 20% smaller than the adopted value of 0.209(6) e^2b^2 [5]. Also, for the $B(E2)$ in ^{112}Sn and ^{114}Sn the observed difference is of the order of 20% (see Table 1). However, remembering that the $B(E2)$ values in ^{112,114}Sn have been deduced in Refs. [12,13] relative to an adopted value for ^{116}Sn, it is interesting to note that renormalization to our new $B(E2)$ value for ^{116}Sn leads to values of $B(E2) = 0.195(8)$ e^2b^2 and $B(E2) = 0.186(8)$ e^2b^2 for ^{112}Sn and ^{114}Sn, respectively, which are then in excellent agreement with our values. Coming back to the conflicting case of ^{116}Sn, it is interesting to note that the adopted $B(E2)$ value quoted in [5] is based on fifteen individual measurements (ranging from 0.145(21) to 0.29(6) e^2b^2) performed between 1957 and 2000 using Coulomb excitation, nuclear resonance fluorescense or electron scattering. While our new values deduced from the measured lifetimes overlap within the experimental uncertainties with eight of them, they clearly deviate from the values obtained in Coulomb excitation experiments, which have the smallest quoted error bars, namely 0.216(5) e^2b^2, 0.195(7) e^2b^2 and 0.223(13) e^2b^2 [22–24], and which dominate the adopted value.

Unfortunately only in three cases, ^{112}Sn, ^{114}Sn and ^{120}Sn, measurements of the 2^+_1 lifetime using Doppler techniques have been

reported in the literature. Using the $(n, n'\gamma)$ reaction and the DSA method, Orce et al. obtained a value of $\tau(2_1^+) = 0.750(^{+125}_{-90})$ ps in ^{112}Sn which later on was corrected to $\tau(2_1^+) = 0.535(^{+100}_{-80})$ ps [10]. Note that, in contrast with the present DSA measurements, those in Ref. [10] have a very low recoil velocity and the measured average Doppler shift is relatively insensitive to nuclear life-times in this time regime. In ^{114}Sn the Cologne group measured $\tau(2_1^+) = 0.56(11)$ ps performing a DDCM (differential decay curve method) coincidence analysis of plunger data [25]. Finally, DSA values of $\tau(2_1^+) = 0.45(15)$ ps for ^{114}Sn and $\tau(2_1^+) = 0.95(6)$ ps for ^{120}Sn have been reported in Refs. [26,27]. All these values agree within the experimental uncertainties with the results of our present work.

The experimental $B(E2)$ values in $^{112–124}$Sn obtained in the present work are compared to literature values in Fig. 3. While the adopted values are smoothly increasing from ^{124}Sn towards the mid-shell nucleus ^{116}Sn, our new results rather seem to indicate a minimum at $N = 66$ followed by a smooth increase between ^{116}Sn and ^{112}Sn. It is important to remember that the new $B(E2)$ values for ^{112,114,116}Sn and ^{116,118,120}Sn, respectively, have been consistently determined under identical conditions in the GSI and ANU experiments. A similar behavior of the $E2$ strength in the upper half of the $N = 50$–82 neutron shell, namely a maximum at ^{120}Sn, has already been observed in a study using nuclear resonance fluorescense techniques [28].

As shown in Fig. 3, there is a very close matching between the observed minimum in transition strengths and the increase in 2_1^+ excitation energies around ^{114,116}Sn. From the theoretical point of view, the consistent description of nuclear properties such as the energy of the first excited 2^+ state or the $B(E2; 0_{g.s.}^+ \rightarrow 2_1^+)$ transition probabilities across the entire span of a large major neutron shell is a very challenging task. In the nuclear shell model a neutron configuration space consisting of all five orbitals between $N = 50$ and $N = 82$, namely $d_{5/2}$, $g_{7/2}$, $s_{1/2}$, $d_{3/2}$ and $h_{11/2}$, is still far too big to be treated in an exact way. In the large-scale shell model calculations presented in Ref. [7], a truncation scheme based on the generalized seniority model was employed. The calculated $B(E2)$ values show a parabolic behavior with a maximum for the mid-shell nucleus ^{116}Sn (see Fig. 3). More recently, however, expanded shell model calculations [11] have for the first time shown deviations from a $B(E2)$ symmetry around mid-shell. This interesting result certainly motivates further theoretical investigation. Besides the shell model calculations other theoretical approaches have recently been used to study the systematic behavior of $E2$ transition strengths in the Sn isotopes. The 2_1^+ energies and $B(E2)$ transition probabilities for all Sn isotopes from $N = 50$ to $N = 82$ have been calculated in a relativistic quasiparticle random phase approximation (RQRPA) [29,30]. In these calculations, which are included in Fig. 3, the transition strength shows a maximum of about 0.24 e^2b^2 around ^{106}Sn/^{108}Sn, decreases with increasing neutron number towards mid-shell and then stays nearly constant around 0.15 e^2b^2 up to ^{124}Sn before it drops again towards ^{130}Sn. Another example are the QRPA calculations of Terasaki [31] which unfortunately only have been performed for the upper half of the major shell. Here the $E2$ strength is maximal for ^{118,120}Sn, in agreement with our observations, with a decreasing trend towards both the lighter and heavier isotopes.

Aspiring to at least a qualitative understanding of the experimental findings, we performed spherical self-consistent Hartree–Fock–Bogoliubov calculations along the isotopic chain employing the Finite Range density-dependent Gogny force. Fig. 4 shows the evolution of the calculated neutron single-particle energies between $N = 50$ and $N = 82$. The degree of collectivity of the first excited 2^+ states is, in general terms, given by the number of avail-
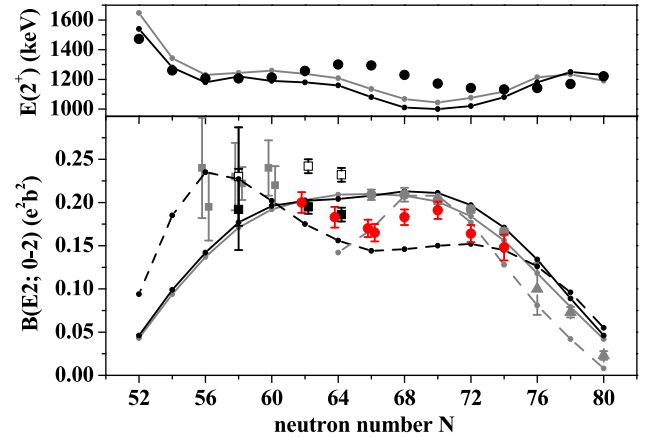

Fig. 3. Experimental 2_1^+ excitation energies [5] (top) and $B(E2)$ values (bottom) as obtained in the present work (red circles) and in Refs. [5–11]. The ^{108,112,114}Sn values from [7,12,13] (open squares) have been renormalized (black squares) using the new experimental $B(E2)$ value for ^{112,116}Sn. The shell model calculations using a ^{100}Sn core and an neutron effective charge of $1.0e$ from [7] and [11] are shown as grey and black lines while the RQRPA [29,30] and QRPA [31] calculations are presented as dashed black and grey lines, respectively.
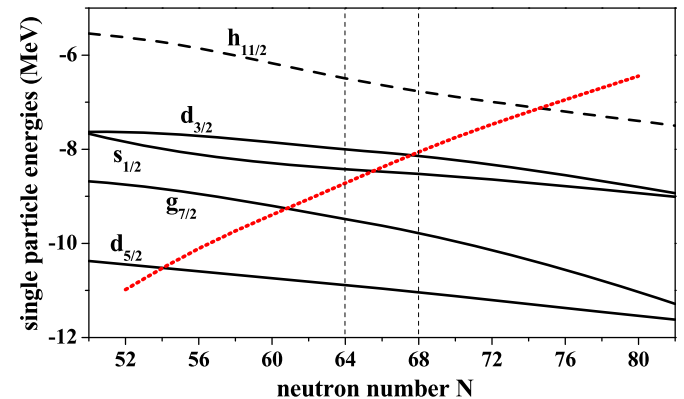

Fig. 4. Evolution of the neutron single-particle energies as a function of the neutron number N along the chain of Sn isotopes. The Fermi level is shown as a thick dotted (red) line. (For interpretation of the references to color in this figure legend, the reader is referred to the web version of this Letter.)

able particle–hole (two-particle or two-hole) excitations close to the Fermi level that can couple to $J^\pi = 2^+$. In this respect, the $s_{1/2}$ orbit plays a distinctive role since a $s_{1/2}$ neutron can contribute to the 2_1^+ state only when coupled to a $d_{3/2}$ neutron (the $d_{5/2}$ orbit is far away in energy), while $s_{1/2}^2$ two-particle or $s_{1/2} \otimes g_{7/2}^{-1}$ particle–hole excitations are excluded. Whereas this peculiarity is unimportant as long as the $s_{1/2}$ orbit is either far above or far below the Fermi level, it has marked consequences when this orbit is close to the Fermi level. The latter is the case in the region $N = 64$–68 (see Fig. 4) with the Fermi level crossing the $s_{1/2}$ sub-shell at $N = 66$ (where actually both the $s_{1/2}$ and the $d_{3/2}$ orbits are half filled, compare Fig. 3 of Ref. [32]). This obstructive effect of the $s_{1/2}$ orbit on collectivity is further enhanced by the low density of single-particle states around the Fermi level, which reduces the probability of pair excitations. In this region, therefore, the detrimental role of the $s_{1/2}$ orbit leads to a reduction in collectivity as reflected in the decrease of the $E2$ strength and the simultaneous increase of the 2_1^+ energies (see Fig. 3).

In conclusion, new experimental $B(E2; 0_{g.s.}^+ \rightarrow 2_1^+)$ transition probabilities based on direct lifetime measurements have been presented for all stable even-A tin isotopes from ^{112}Sn to ^{124}Sn. A shallow minimum is observed for the mid-shell isotope ^{116}Sn.

Its origin has been ascribed to the obstructive effect of the $s_{1/2}$ orbital, which is close to the Fermi level in this region, and inhibits collectivity. While the new experimental results are in contrast to the seniority truncated large-scale shell model calculations, which predict a maximum of the $E2$ strength at $N = 66$ [7], expanded shell model calculations employing new interactions [11] indicate a shallow maximum around $N = 68$–70, closer to the experimental findings. New insight into the proton and neutron composition of the nuclear wave functions is awaited from the determination of the magnetic moments of the 2_1^+ states from the same data set [15] which may elucidate the interplay between single particle and collective degrees of freedom.

We hope that our new experimental results for the stable Sn isotopes will stimulate new theoretical studies as well as new experiments to improve and extend the $B(E2)$ measurements on the neutron-deficient radioactive isotopes.

Acknowledgements

References

[1] D. Seweryniak, et al., Phys. Rev. Lett. 99 (2007) 022504.
[2] A. Jungclaus, et al., Phys. Rev. Lett. 99 (2007) 132501.
[3] T.R. Rodríguez, J.L. Egido, A. Jungclaus, Phys. Lett. B 668 (2008) 410.
[4] I. Talmi, Simple Models of Complex Nuclei, Harwood Academic Publishers, 1993.
[5] S. Raman, C.W. Nestor, P. Tikkanen, At. Data Nucl. Data Tables 78 (2001) 1.
[6] D.C. Radford, et al., Nucl. Phys. A 746 (2004) 83c.
[7] A. Banu, et al., Phys. Rev. C 72 (2005) 061305(R).
[8] J. Cederkäll, et al., Phys. Rev. Lett. 98 (2007) 172501.
[9] C. Vaman, et al., Phys. Rev. Lett. 99 (2007) 162501.
[10] J.N. Orce, et al., Phys. Rev. C 76 (2007) 021302(R);
J.N. Orce, et al., Phys. Rev. C 77 (2008) 029902(E).
[11] A. Ekström, et al., Phys. Rev. Lett. 101 (2008) 012502.
[12] P. Doornenbal, et al., Phys. Rev. C 78 (2008) 031303(R).
[13] R. Kumar, et al., Phys. Rev. C 81 (2010) 024306.
[14] M. East, et al., Phys. Lett. B 665 (2008) 147.
[15] J. Walker, A. Jungclaus, et al., in preparation.
[16] J.C. Wells, N.R. Johnson, computer code LINESHAPE, ORNL, 1994.
[17] J.F. Ziegler, J.P. Biersack, U. Littmark, in: J.F. Ziegler (Ed.), The Stopping and Range of Ions in Solids, in: The Stopping and Ranges of Ions in Matter, vol. 1, Permagon, New York, 1985.
[18] N.-G. Jonsson, et al., Nucl. Phys. A 371 (1981) 333.
[19] L.I. Govor, et al., Yad. Fiz. 54 (1991) 330, Sov. J. Nucl. Phys. 54 (1991) 196.
[20] L.C. Northcliff, R.F. Schilling, Nucl. Data Tables A 7 (1970) 233.
[21] A. Jungclaus, et al., in preparation.
[22] P.H. Stelson, F.K. McGowan, R.L. Robinson, W.T. Milner, Phys. Rev. C 2 (1970) 2015.
[23] R. Graetzer, S.M. Cohick, J.X. Saladin, Phys. Rev. C 12 (1975) 1462.
[24] A.M. Kleinfeld, R. Covello-Moro, H. Ogata, G.G. Seaman, S.G. Steadman, J. de Boer, Nucl. Phys. A 154 (1970) 499.
[25] J. Gableske, A. Dewald, H. Tiesler, M. Wilhelm, T. Klemme, O. Vogel, I. Schneider, R. Peusquens, S. Kasemann, K.O. Zell, P. von Brentano, P. Petkov, D. Bazzacco, C. Rossi Alvarez, S. Lunardi, G. de Angelis, M. de Poli, C. Fahlander, Nucl. Phys. A 691 (2001) 551.
[26] I.N. Vishnevsky, M.F. Kudoyarov, E.V. Kuzmin, Yu.N. Lobach, A.A. Pasternak, V.V. Trishin, Program and Thesis, Proc. 41. Ann. Conf. Nucl. Spectrosc. Struct. At. Nuclei, Minsk (1991) 71.
[27] S.H. Sie, J.S. Geiger, R.L. Graham, D. Ward, H.R. Andrews, AECL-4147 (1972) 14.
[28] J. Bryssinck, et al., Phys. Rev. C 61 (2000) 024309.
[29] A. Ansari, Phys. Lett. B 623 (2005) 37.
[30] A. Ansari, P. Ring, Phys. Rev. C 74 (2006) 054313.
[31] J. Terasaki, Nucl. Phys. A 746 (2004) 583c.
[32] M. Anguiano, J.L. Egido, L.M. Robledo, Phys. Lett. B 545 (2002) 62.